



LAWRENCE
LIVERMORE
NATIONAL
LABORATORY

Tunable Plasmonic Nanogap Resonator

T. Bond, M. Bora, A. Chang, R. Miles

June 21, 2012

the 6th International Conference on Nanophotonics
Rome, Italy, Italy
August 18, 2012 through August 25, 2012

Disclaimer

This document was prepared as an account of work sponsored by an agency of the United States government. Neither the United States government nor Lawrence Livermore National Security, LLC, nor any of their employees makes any warranty, expressed or implied, or assumes any legal liability or responsibility for the accuracy, completeness, or usefulness of any information, apparatus, product, or process disclosed, or represents that its use would not infringe privately owned rights. Reference herein to any specific commercial product, process, or service by trade name, trademark, manufacturer, or otherwise does not necessarily constitute or imply its endorsement, recommendation, or favoring by the United States government or Lawrence Livermore National Security, LLC. The views and opinions of authors expressed herein do not necessarily state or reflect those of the United States government or Lawrence Livermore National Security, LLC, and shall not be used for advertising or product endorsement purposes.

Tunable Plasmonic Nanogap Resonator

Tiziana C. Bond, Mihail Bora, Allan Chang,
Center of Micron and Nano Technology
Lawrence Livermore National Laboratory
Livermore, USA
e-mail: bond7@llnl.gov

Abstract—We present a new class of plasmonic substrates based on lithographically-defined two-dimensional rectangular array of nanopillars over very large areas (4" wafers). For these vertical nanopillars, the gap between each pair of neighboring nanopillars is small enough (< 100 nm) that highly confined plasmonic cavity resonances are supported in between such pairs. The resonant structures are tunable the 400-800nm visible range with strong field enhancements and absorbance up to 80%; we discuss of their potential extension to ultra-violet and infrared ranges with maximum absorbance $> 95\%$ at resonance due to a highly efficient coupling with incident light. Because of their design flexibility these nanotemplates they can impact various areas, from detection and spectroscopy to energy harvesting to photovoltaic.

Keywords—component; plasmonics; resonant cavity; tunability; nanolithography

I. INTRODUCTION

Plasmonic nanostructures are being widely investigated due to their strong controllability potential which suite their exploitation in disparate fields from bio-molecular detection [1-3] to sub-wavelength optics [4-6] and photovoltaic technology [7-9], to just name a few. A plethora of geometries have been employed but typically offer enhancements over narrow wavelength and incident angle ranges [10-14]. There are currently new efforts in overcoming this inherent limitation of plasmonic nanostructures [ref to double shells and others]. Here we propose a controllable broadband, tunable platform in which vertical plasmon resonant nanocavities are arranged in uniform and dense arrays of coupled metallic nanowires, over large area substrates [ref to other nanoletter paper]. Tuning and broadening of the plasmonic multiple resonances is obtained by controlling the geometrical dimensions of the cavity, i.e nanowire gaps and heights, or the optical properties of the environment, i.e. the dielectric constant. In particular, the vertical dimension dictates the supported wavelength resonances and total span as supposed in a Fabry-Perot type resonant cavity, whereas the horizontal dimensions is responsible for the quality factor of the cavities, in other words the width and strength of the resonances. Using such knobs, UV to IR spectrum can be covered at once with less or more resonant prominent plasmonic features favoring the conditions for either specific wavelength alignment as needed in spectroscopy or widely absorbing plasmons more critical in energy harvesting applications. Furthermore, because of the square lattice

arrangement of the pillars, the platform is also polarization independent which can be advantageous as it reduces requirements of the available sources.. In the following we will in particular discuss about the technology providing high density tunable plasmonic paired nanopillars with excellent control of the cavity size over a very large area (4 inch wafer) and uniform substrate. Tuning of the plasmon resonance in the 500-800 nm range is demonstrated by controlling the geometrical dimensions of the cavity and the dielectric environment. The reflectivity and absorbance of the arrays of cavities for gold, silver and aluminum metals are presented. The limitations for the implementation of such a structure are discussed nevertheless showing that the visible averaged absorbance can be increased above 80%, a remarkable feature considering that these metals are used to fabricate highly reflective optical mirrors.

II. EXPERIMENTS

A. Fabrication of Nanopillar Templates

The plasmonic substrate is composed of a rectangular array of vertical nanopillars coated with gold, silver or aluminum, The fabrication steps are reported in Fig.1

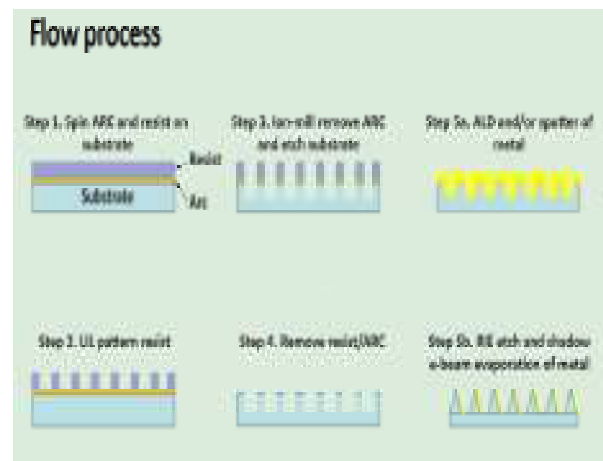


Figure 1. Fabrication steps details.

The period of the array is 360 nm, chosen such that no diffraction grating effects take place in the visible spectrum under normal incidence.. The nanopillar array template is patterned using laser interference lithography [14] over 4-

inch fused silica wafers that are coated with half-micron thick photoresist. The laser wavelength for the holography is 413 nm and the dose $\sim 40 \text{ mJ/cm}^2$. The resultant photoresist structure is a periodic array of pillars with pitch of 360 nm and diameter ranging between 130 - 150 nm due to source dose variation. The patterned photoresist acts as the etching mask in a subsequent step of ion beam milling which enables the transfer of the geometry into a silicon or fused silica substrate. Further, the structure is either sputtered with a conformal metallic film using a chromium adhesion layer or coated with a thick layer of Al_2O_3 by Atomic Layer Deposition (ALD) followed by a subsequent step of conformal sputtering of thinner metal layers. In this context we will discuss only the results obtained with just conformal the former step as it would give more flexibility in controlling the aspect ratio of height vs. gap (or diameter of the pillars) due to the different vertical vs. sidewall deposition rates, eventually resulting more amenable to the desired tunability. In fact, the height and diameter of the pillars is determined by the etch time and sputtering time respectively as shown in Figs. 2a and 2b. Incidentally, the combined ALD/sputtering process becomes more appealing for applications that require much smaller gaps ($< 10 \text{ nm}$) such as Surface Enhanced Raman Spectroscopy, as it helps in tightening the control at the atomic level [REF]. Pairs of vertically aligned nanopillars form a metal-dielectric-metal waveguide when the edge to edge separation is closer than 100 nm (Fig. 2c). Plasmon modes are excited by normal incident light waves in the transverse magnetic (TM) polarization mode.

B. *Plasmonic Resonance Cavity Model*

The resonant modes of the cavity are formed by the interference of forward and backward propagating waves and are determined by the dispersion relation of the waveguide and the phase shifts at each end

$$2k_{sp}h + \varphi_1 + \varphi_2 = 2m\pi, \quad (1)$$

where k_{sp} is the wavevector of the surface plasmon wave, h is the length of the cavity, φ_1 and φ_2 , are the phase changes at the top and bottom boundaries and m is the resonance order. The dispersion relation, $k_{sp}(\omega)$ can be approximated with that of a semi-infinite planar metal-dielectric-metal waveguide or calculated analytically. Fig. 2d shows the electric field amplitude profile for a resonant mode of order $m = 4$, as seen from three orthogonal cross sections. The node and anti-node conditions at each end correspond to phase shifts of 0 and $\pi/2$, however, these values can be corrected to more accurate values dependent on the real waveguide geometry and dielectric medium. In Fig. 2e we highlight the tangential power flow for the $m = 4$ mode. A net power flow occurs in the horizontal directions only at the rounded tapered region corresponding to a lateral flow convergent into the inter-wire waveguide. The curved ending acts as a sub-wavelength electromagnetic lens that

effectively increases the absorbance cross section of the cavity.

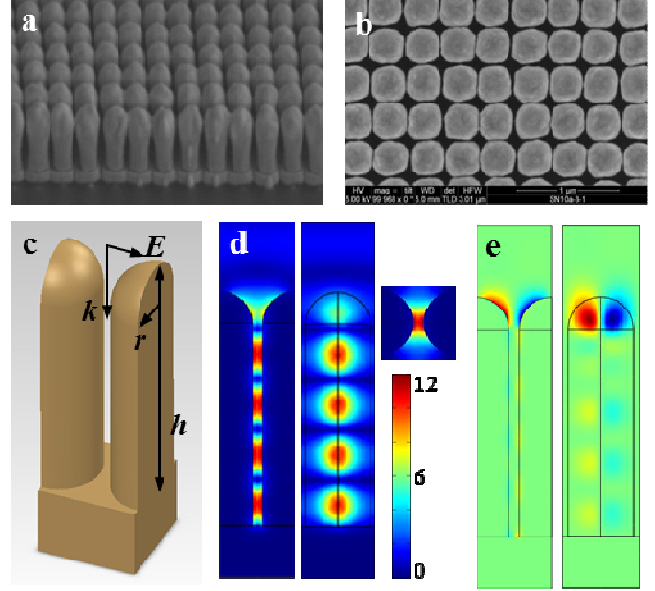


Figure 2. Scanning electron micrographs of the vertical metallic nanopillars viewed from side (a) and top (b). (c) Unit cell of the rectangular array centered on the plasmon nanocavity. The geometry of the array is specified by the pitch, radius and height of the pillars. The nanocavity is optically excited with normal incidence light, polarized in the transverse magnetic mode d, Simulations of the electric field amplitude in the resonator seen from front, side and top. (e) Tangential power flow in the vertical symmetry planes of the cavity highlights the electromagnetic energy channeling into the inter-pillar region from the top of the cavity.

C. *Characterization and Model Validation*

The frequency response of the resonator shows strong absorbance peaks that correspond to excitation of high electric field amplitude modes. The overall absorbance can be increased by adjusting the length of the resonator such that additional higher order modes are excited. Fig. 3 represents the simulated and experimentally measured reflectance of an array with 360 nm pitch made of silver nanopillars of 300 nm diameter and 1000 nm height. The electric field amplitude profile of the mode on the vertical symmetry axis of the unit cell is plotted as a function of wavelength. The plasmon cavity resonates at all frequencies, however the strongest field enhancements are observed for the modes that extend further into the free space and have a better overlap with the incident photon field. Interestingly, weak plasmon modes are excited even for conditions that correspond to reflectivity maxima, suggesting that engineering the shape of the coupling end can lead to even stronger absorbance of the array over the whole spectrum.

Array reflectivities were calculated for nanopillar arrays of variable height made of three metals arranged in the increasing order of their bulk plasma frequency: gold (8.55

eV), silver (9.6 eV) and aluminum (15.3 eV). The gold is significant for bio-molecular sensing, while silver and aluminum are relevant for photovoltaic applications since resonances have a better overlap with the solar spectrum.

In Figure 4 we show the simulated reflectance spectrum of 360 nm pitch array of vertical nanowires of diameter 310 nm, variable height h , and capped by a hemisphere of diameter 310 nm. In the case of gold only a fraction of the visible spectrum is covered by plasmon resonances as the cut off frequency corresponds to an excitation wavelength of 550 nm, while for silver and aluminum the entire visible spectrum is covered. As the height of the pillar is increased the spacing between consecutive modes is decreasing enabling the cavity to have a strong absorbance at more excitation wavelengths. The simulations for the aluminum structures suggest that past a certain height, an increase in the length of the resonator causes a decrease in the absorbance strength. This can be explained by the higher losses of aluminum combined with longer paths of the plasmon at the interfaces. Alternatively, the effective length of the resonator can be changed by increasing the refractive index of the dielectric core.

The effectiveness of the resonant array as a broadband absorber was assessed by calculating the average absorbance of the array in the 400-800 nm spectral range as a function of nanopillar height (Fig. 5). A stepwise decrease in absorbance is observed each time an additional resonance is added to the reflectance spectrum of the array. The absorbance of the array is referenced to the average reflectivity for flat films: 80% for gold, 95% for silver and 90% for aluminum. Experimental data points for fabricated samples are superimposed on the absorbance plot.

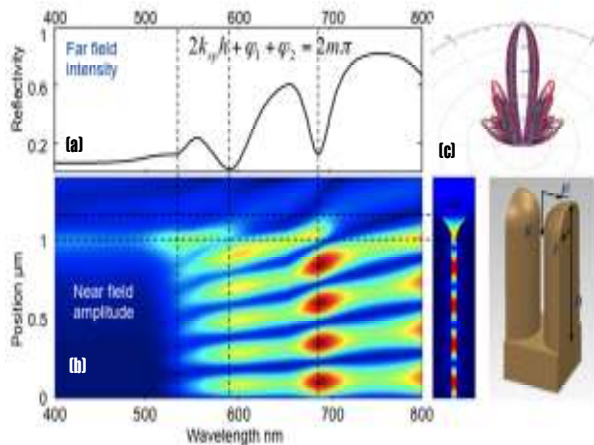


Figure 3. (a) Normal incidence reflectance (simulation and experiment) for a gold nanocavity 1000 nm long, 60 nm wide, showing full resonances of order 4, and 5. (b) Electric field amplitude of the plasmon mode in the center of the cavity plotted as a function of position and excitation wavelength. (c) Radar mapping showing directionality of the nanopyllar antennae.

The averaged absorbance becomes larger than the values calculated in Figure 5.a when restricted to a frequency range

above common semiconductor bandgaps and when weighted by the photon energy and the solar irradiance spectrum. If the refractive index of the inter-wire dielectric core is increased, the cutoff plasma frequency and the plasmon resonance locations are red shifted and the spacing between resonances becomes smaller as the optical length of resonator is increased. Based on these arguments, aluminum nanowire dielectric hybrid structures have a better spectral coverage than any other metal considered. Silver on the other hand has the lowest losses in the visible and it is most efficient for transferring energy from the plasmon modes into the absorptive dielectric material. The gold nanowire arrays have a significant potential for biological sensing.

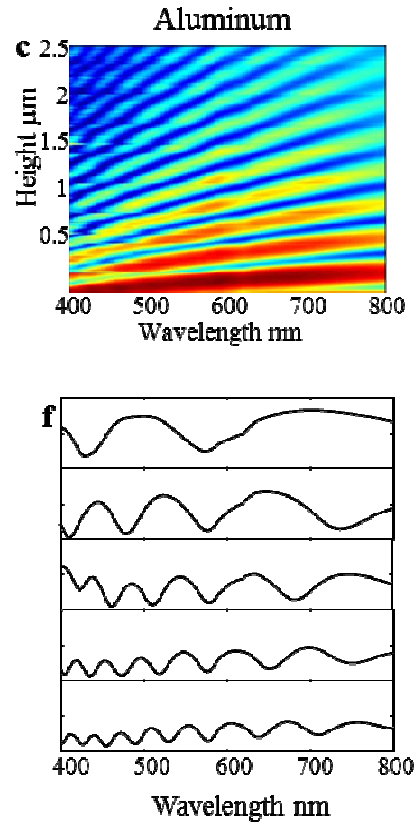


Figure 4. Simulations of the normal incidence reflected power for aluminum (c) as a function of wavelength and nanowire height (label the plot with the metal). Multiple resonances can be excited below the plasmon cutoff frequency. Experimental plots of reflectivity for flat metallic films and nanowire arrays of height equal to 0.5, 1, 1.5, and 2 μm for gold (d), silver (e) and aluminum (f). In all plots the reflectivity scale is 0 to 1.

III. CONCLUSIONS

We demonstrated multiresonant plasmonic nanocavities in vertical metallic nanopillar arrays with strong overlap and coupling between incident light and the plasmon modes. The absorbance of nanostructured metallic surfaces has been

engineered to cover multiple wavelengths by increasing the longitudinal dimensions of the plasmon resonant nano-cavities. For large cavity sizes for aluminum and longer for silver and gold, the benefit of multiple resonances is offset by the weaker coupling into plasmons as the round trip losses in the cavity become significant enough to decrease the electric field amplitude of the modes. Using geometry dependent tuning, the resonances can be further optimized for renewable energy applications for a better overlap with the absorbance of semiconductor materials. Most of the incident light is reflected in the red side of the spectrum, as the resonance spacing is increased at longer wavelengths.

Finally, in terms of application we need to mention that the nano-cavities are envisioned in high sensitivity Raman spectroscopy that requires high local electromagnetic fields and alignment between the plasmon resonance and excited and scattered light [REF]. The tunable nanocavity will be of particular relevance for fabrication of plasmonic lasers which use surface plasmons instead of light to pump the lasing medium [REF]. Since the device structure relies on vertical free standing nano-wires the plasmonic cavity region can be filled with any material of choice. Therefore, in addition to the high confinement factors shown, the cavity plasmon resonance can be adjusted for maximum overlap with the absorbance of the active material

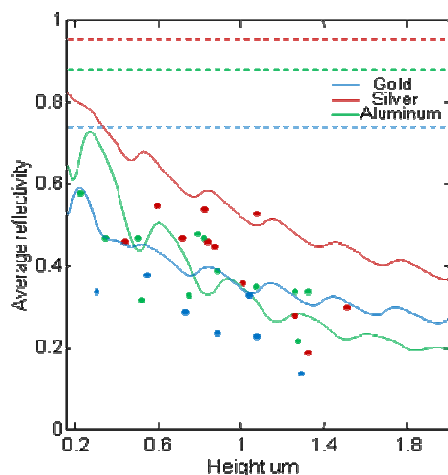


Figure 5. Average absorbance. Lines are simulations results; dots are data points. The discrepancy is mainly due to the deviation from the ideal straight cylinder shapes of the real fabricated devices. Dotted lines represent the reflectivity of smooth thin film of each metals.

ACKNOWLEDGMENT

Acknowledgment. The authors thank Cindy Larson, and Jerry Britten for helping patterning the samples, Nick Teslich and Ed Sedillio on the preparation of the SEM samples. This work was performed under the auspices of the U.S. Department of Energy by Lawrence Livermore National Laboratory under Contract DE-AC52-07NA27344. LLNL- JRNL-425128.

REFERENCES

- [1] Hirsch, L. R.; Jackson, J. B.; Lee, A.; Halas, N. J.; West, J. *Analytical Chemistry* 2003, 75, 2377.
- [2] Rich, R. L.; Myszka, D. G. *Current Opinion in Biotechnology* 2000, 11, 54.
- [3] Bora, M.; Celebi, K.; Zuniga, J.; Watson, C.; Milaninia, K. M.; Baldo, M. A. *Optics Express* 2009, 17, 329.
- [4] Barnes, W. L.; Dereux, A.; Ebbesen, T. W. *Nature* 2003, 424, 824.
- [5] Ghaemi, H. F.; Thio, T.; Grupp, D. E.; Ebbesen, T. W.; Lezec, H. J. *Physical Review B* 1998, 58, 6779.
- [6] Lezec, H. J.; Degiron, A.; Devaux, E.; Linke, R. A.; Martin-Moreno, L.; Garcia-Vidal, F. J.; Ebbesen, T. W. *Science* 2002, 297, 820.
- [7] Morfa, A. J.; Rowlen, K. L.; Reilly, T. H.; Romero, M. J.; van de Lagemaat, J. *Applied Physics Letters* 2008, 92.
- [8] Tvingstedt, K.; Persson, N. K.; Ingnas, O.; Rahachou, A.; Zozoulenko, I. V. *Applied Physics Letters* 2007, 91.
- [9] Westphalen, M.; Kreibitz, U.; Rostalski, J.; Luth, H.; Meissner, D. *Solar Energy Materials and Solar Cells* 2000, 61, 97.
- [10] Odom T., *Nature Nanotechnology* 2010
- [11] Schuck, *Nanotechnology* 2010
- [12] Jn Zhang
- [13] Kubo, N. and Fujikawa S., *Nanotechnology* 2011, 11,8

